Supporting Information

For

Rapid C-H Bond Activation by a Monocopper(III)-Hydroxide Complex

Patrick J. Donoghue,[1] Jacqui Tehranchi,[1] Christopher J. Cramer,[1] Ritimukta Sarangi,[2] Edward I. Solomon,[2,3] and William B. Tolman[1,*]

[1]Department of Chemistry, Center for Metals in Biocatalysis, and Supercomputer Institute, University of Minnesota, 207 Pleasant St. SE, Minneapolis, MN 55455 [2]Stanford Synchrotron Radiation Lightsource, SLAC National Accelerator Laboratory, Menlo Park, CA 94025 [3]Department of Chemistry, Stanford University, Stanford, CA 94305.

Experimental Details

General. All chemicals were purchased from Aldrich and used without purification unless listed below. Spectroscopic grade acetone was degassed and dried over activated 3 Å molecule sieves for a minimum of two days then distilled under vacuum. Purified acetone was stored in a nitrogen filled glove box and filtered through a 0.45 μm PTFE syringe filter immediately before use. Dihydroanthracene was recrystallized from ethanol. *N,N*'-Bis(2,6-diisoproylphenyl)-2,6-pyridinedicarboxamide[1], tris(p-tolyl)ammonium hexafluorophosphate ((p-tolyl)$_3$NPF$_6$)[2], and d$_4$-dihydroanthracene[3] were prepared as previously described.

Physicial methods. UV-vis spectra were collected on a HP8453 (190-1000 nm) diode array spectrophotometer. Low temperature UV-vis experiments were performed using a Unisoku low temperature UV-vis cell holder. In the event of minimal frosting in the low temperature cell holder, baseline corrections were performed by subtracting an average region of no absorbance from the spectra (950-980 nm). GC-MS analysis was performed using an Agilent Technologies 7890A GC system and 5975C VL MSD. Elemental analyses were performed by Robertson Microlit Laboratory (Ledgewood, NJ). Infrared spectra were collected on a Nicolet Avatar 370 FT-IR equipped with a Smart OMNI Sampler. EPR data was collected on a Bruker Elexsys E500 spectrometer using X-band radiation at 2 K. Simulations were performed using Bruker SimFonia software (version 1.25).

X-ray Absorption Spectroscopy. The Cu K-edge X-ray absorption spectra of [Bu$_4$N][**2**], [Bu$_4$N][**3**], and **4** were measured at the Stanford Synchrotron Radiation Lightsource (SSRL) on the 20 pole, 2 T wiggler beamline 7-3 under standard ring conditions of 3 GeV and ~300 mA ring current. A Si(220) double-crystal monochromator was used for energy selection. Other optical components used for the experiments were a cylindrical Rh-coated bent focusing mirror. Spectra were collected in the fully tuned configuration of the monochromator. The solution samples were immediately frozen after preparation and stored under liquid N_2 until measurement. During data collection, the samples were maintained at a constant temperature of ~10 K using an Oxford Instruments CF 1208 liquid helium cryostat. Data were measured to k=14 Å^{-1} by using a Canberra Ge 30-element array detector. Internal energy calibration was accomplished by simultaneous measurement of the absorption of a Cu-foil placed between two ionization chambers situated after the sample. The first inflection point of the foil spectrum was fixed at 8980.3 eV. The samples were monitored for photoreduction and to minimize the effect of beam damage, a single spectrum was obtained from each sample spot. A total of 8 sample spots were exposed and the data presented here are 8 scan average spectra for all samples. The data were processed by fitting a second-order polynomial to the pre-edge region and subtracting this from the entire spectrum as background. A four-region spline of orders 2, 3, 3 and 3 was used to model the smoothly decaying post-edge region. The data were normalized by subtracting the cubic spline and assigning the edge jump to 1.0 at 9000 eV using the Pyspline program.[4] Theoretical EXAFS signals $\chi(k)$ were calculated by using *FEFF* (Macintosh version 8.4)[5-7] and

(1) Wasilke, J.-C.; Wu, G.; Bu, X.; Kehr, G.; Erker, G. *Organometallics* **2005,** *24,* 4289.
(2) Manner, V. W.; DiPasquale, A. G.; Mayer, J. M. *J. Am. Chem. Soc.* **2008**, *130*, 7210.
(3) Goldsmith, C. R.; Jonas, R. T.; Stack, T. D. P. *J. Am. Chem. Soc.* **2002**, *124*, 83.
(4) Tenderholt, A. *Pyspline and QMForge*, 2007.
(5) Rehr, J. J.; Albers, R. C. *Rev. Mod. Phys.* **2000**, *72*, 621-654.
(6) Rehr, J. J.; Mustre de Leon, J.; Zabinsky, S. I.; Albers, R. C. *J. Am. Chem. Soc.* **1991**, *113*, 5135-5140.
(7) Mustre de Leon, J.; Rehr, J. J.; Zabinsky, S. I.; Albers, R. C. *Phys. Rev. B: Condens. Matter* **1991**, *44*, 4146-4156.

the crystal structure of [PPN][**2**] and [PPN]**3** and a structural model of **4** made using Avogadro. The theoretical models were fit to the data using EXAFSPAK.[8] The structural parameters varied during the fitting process were the bond distance (R) and the bond variance σ^2, which is related to the Debye-Waller factor resulting from thermal motion, and static disorder of the absorbing and scattering atoms. The non-structural parameter E_0 (the energy at which k=0) was also allowed to vary but was restricted to a common value for every component in a given fit. Coordination numbers was systematically varied in the course of the fit but were fixed within a given fit.

[N,N'-Bis(2,6-diisoproylphenyl)-2,6-pyridinedicarboxamido]acetonitrilecopper(II) (LCu(CH_3CN), 1): The title compound was prepared using a modified procedure to the one previously described.[9] Into a 100 mL round bottom flask was placed bis(2,6-diisopropylphenyl)pyridine-2,6-dicarboxamide (0.487 g, 1.00 mmol) and copper(II) triflate (0.346 g, 0.96 mmol). The solids were dissolved in 50 mL of MeOH forming a pale green solution. Sodium methoxide (0.5 M in methanol, 4.00 mL, 2.00 mmol) was then added causing the solution to immediately turn deep green. The solution was stirred at room temperature for 10 min, after which the solvents were removed *in vacuo*. The dark green residue was dissolved in 50 mL CH_3CN, forming a mahogany solution. The solvents were again removed *in vacuo* and the residue dissolved in 50 mL CH_2Cl_2 and filtered to remove sodium triflate. The remaining solution was evaporated and the solids dissolved in a minimum of CH_3CN (20 mL) diluted with toluene (80 mL) and placed in the freezer overnight whereupon dark mahogany crystals formed. The crystalline solid was isolated by filtration and dried *in vacuo* (0.446 g, 79.2%). Crystals suitable for X-ray diffraction were prepared by slow evaporation of an acetonitrile solution of the product at -30 °C to give deep red blocks. Analytical data matched previously reported values.[9]

Tetrabutylammonium [N,N'-Bis(2,6-diisoproylphenyl)-2,6-pyridinedicarboxamido] copper(II) chloride ([Bu_4N][LCuCl], [Bu_4N][2]): To a solution of **1** (147.9 mg, 0.25 mmol) in THF (15 mL) was added Bu_4NCl (70.0 mg, 0.25 mmol). The solution was stirred at room temperature for 30 min during which time it turned deep green. The solvent was then removed *in vacuo*. The residual green solid was suspended in 15 mL of Et_2O, stirred for 30 min and evaporated (3x) to help remove residual THF. The powdery solid was then suspended in 15 mL Et_2O and allowed to stir overnight. The solution was then filtered, the collected solids were washed with an additional 10 mL Et_2O, and then further dried *in vacuo* overnight to yield the product as a green powder (166.4 mg, 80.2%). Crystals suitable for X-ray diffraction were prepared by adding one equivalent of PPNCl to **1** in THF, followed by vapor diffusion of hexanes at −30 °C to yield bright green needles. UV-vis (acetone, −80 °C) λ_{max}, nm (ε): 400 (3330), 625 (432). Anal. Calcd for $C_{47}H_{73}ClCuN_4O_2$: C, 68.42; H, 8.92; N, 6.79; Cl, 4.30. Found: C, 68.31; H, 9.32; N, 6.63; Cl, 4.77.

Tetrabutylammonium [N,N'-Bis(2,6-diisoproylphenyl)-2,6-pyridinedicarboxamido] copper(II) hydroxide ([Bu_4N][LCuOH], [Bu_4N][3]): To a suspension of **1** (146.7 mg, 0.25 mmol), in Et_2O (15 mL) was added 0.25 mL of Bu_4NOH solution in MeOH (1.0 M, 0.25 mmol). A blue precipitate formed immediately. The solution was stirred at room temperature for 30 min, after which the solvents were removed *in vacuo*. The residual solids were suspended in 15 mL of Et_2O, stirred for 30 min and evaporated (2x) to help remove any residual MeOH. The powdery solid was then suspended in 15 mL Et_2O and allowed to stir overnight. The mixture was then

(8) George, G. N. *EXAFSPAK and EDG-FIT*, 2000.
(9) Donoghue, P. J.; Gupta, A. K.; Boyce, D. W.; Cramer, C. J.; Tolman, W. B. *J. Am. Chem. Soc.* **2010**, *132*, 15869.

filtered, the collected solids were washed with an additional 10 mL Et_2O, and then further dried *in vacuo* overnight to yield the product as a blue powder (150.5 mg, 74.8%). Crystals suitable for X-ray diffraction were prepared by adding 1 equivalent of PPNCl to a solution of [Bu_4N][**3**] in THF followed by vapor diffusion of hexanes at −30 °C to yield deep blue needles. UV (acetone, -80 °C) λ_{max}, nm (ε): 360 (sh, 2807), 592 (397). Anal. Calcd for $C_{47}H_{74}CuN_4O_3$: C, 69.98; H, 9.25; N, 6.95. Found: C, 69.23; H, 9.18; N, 6.83.

[N,N'-Bis(2,6-diisoproylphenyl)-2,6-pyridinedicarboxamido]aquacopper(II) (LCu(OH$_2$), 5): This complex was prepared via a procedure similar to that used for the synthesis of **1**. Into a 100 mL round bottom flask was placed bis(2,6-diisopropylphenyl)pyridine-2,6-dicarboxamide (0.4861 g, 1.00 mmol) and copper(II) triflate (0.3456 g, 0.96 mmol). The solids were dissolved in 50 mL of MeOH forming a pale green solution. Sodium methoxide (0.5 M in MeOH, 4.0 mL, 2.00 mmol) was then added causing the solution to immediately turn deep green. The solution was stirred at room temperature for 10 min, after which the solvents were removed *in vacuo*. The dark green residue was dissolved in 50 mL CH_3CN, forming a mahogany solution. The solvent was again removed *in vacuo* and the residue dissolved in 50 mL CH_2Cl_2 and filtered to remove sodium triflate. The solvent was evaporated and the solid residue was dissolved in 10 mL of acetone and 10 mL H_2O. The solvents were evaporated, and the residue dissolved in 20 mL of the 1:1 acetone/water mixture twice more to ensure complete removal of CH_3CN. The solvents were evaporated to yield a purple solid that was dried *in vacuo* to yield the product as a dark brown powder (0.4878 g, 86.3%). Crystals suitable for X-ray diffraction were prepared by the slow evaporation of an acetone solution of the brown powder at −30 °C to give brown needles. UV (acetone, -80 °C) λ_{max}, nm (ε): 398 (3067), 558 (692). Anal. Calcd for $C_{31}H_{39}CuN_3O_3$: C, 65.88; H, 6.95; N, 7.43. Found: C, 66.36; H, 6.80; N, 7.50.

Procedure for the oxidation of [Bu$_4$N][LCuOH], [Bu$_4$N][3]: All reactions involving chemical oxidants were performed either in a nitrogen filled glove box or in septum sealed Schlenk flasks under nitrogen or argon. For a typical reaction monitored by UV-vis spectroscopy, 3 mM stock solutions of [Bu_4N][**3**] and ferrocenium hexafluorophosphate ($FcPF_6$) were prepared in acetone. A 0.1 mL aliquot of the stock solution of [Bu_4N][**3**] was added to a UV-vis cuvette along with 2.8 mL of acetone. After cooling the cuvette to −80 °C, 0.1 mL of the $FcPF_6$ solution was added, causing the immediate formation of an intensely purple species (note: after the addition of the oxidant, the cuvette held 3 mL of a solution that was 0.1 mM in Cu). For reactivity studies with DHA, fluorene or diphenylmethane, the appropriate amount of substrate (10 to 2000 equivalents) was added to the cuvette along with [Bu_4N][**3**] prior to cooling to the appropriate temperatures or addition of the oxidant. EPR samples were prepared by injecting a 0.1 mL aliquot of a stock solution (2 mM) of [Bu_4N][**3**] into a quartz EPR sample tube and cooling to −78 °C in a dry ice/acetone bath. A 0.1 mL aliquot of a $FcPF_6$ stock solution (2 mM) was then added. The solution was mixed using a cannula as a stir rod and then the sample was frozen in liquid nitrogen for storage and analysis. Samples for XAS analysis were prepared by adding 0.8 mL of a 12.5 mM solution of [Bu_4N][**3**] to a Schlenk flask. The solution was cooled to −78 °C in a dry ice/acetone bath whereupon 0.2 mL of a 50 mM solution of (p-tolyl)$_3$NPF$_6$ was added. An aliquot of this solution (0.3 mL) was then transferred to an XAS sample cell that was buried in dry ice via a syringe cooled in the dry ice/acetone bath. The sample was then immediately frozen in liquid nitrogen for analysis. (Note: The aminium oxidant was used for the XAS samples due to a complicating side reaction of the oxidized product prepared from $FcPF_6$ with CO_2 (under investigation). UV-vis spectroscopic data showed that the same intermediate formed regardless of the choice of oxidant used.

Cu K-edge XAS and EXAFS Analysis of [Bu_4N][3] and 4. The normalized Cu K-edge XAS spectra of [Bu_4N][**3**] and **4** are shown in the main manuscript (Figure 3). The weak pre-edge transition observed below the onset of the rising-edge occurs due to an electric dipole-forbidden quadrupole-allowed 1s→3d transition. The energy position of the pre-edge transition is dominantly affected by the strength of the ligand field, which reflects the Z_{eff} on the Cu center.[10] For a Cu(II) complex this transition typically occurs at ~8979 eV and is shifted up by ~ 2 eV for a Cu(III) complex (~8981 eV).[11] The pre-edge transition in [Bu_4N][**3**] and **4** occur at 8979.1 eV and 8980.8 eV, respectively clearly showing a 1.7 eV shift on going from [Bu_4N][**3**] to **4** (Table S2). For a given ligand system, the Cu K- rising-edge shifts to higher energy with oxidation state. The rising edge maximum for [Bu_4N][**3**] and **4** occur at 8999.3 and 9000.4 eV, respectively, indicating a 1.1 eV shift on going from [Bu_4N][**3**] to **4**. The shift to higher energy observed in both the pre-edge and rising-edge region clearly indicate that [Bu_4N][**3**] is a Cu(II) species whereas **4** is a one electron oxidized Cu(III) species.

A comparison of the k^3 weighted Cu K-edge EXAFS for [Bu_4N][**3**] and **4** along with their non-phase shift corrected Fourier transforms (k=2-13.2 Å^{-1}) is shown in Figure S6. *FEFF* fits to the data are presented in Figures S7 and S8 and Table S3. On going from [Bu_4N][**3**] to **4**, the EXAFS beat pattern shifts to higher k and the first shell Fourier transform peak intensity increases and shifts to lower R'. This indicates a decrease in first shell bond distances in **4**. *FEFF* fits reveal 4 Cu-N/O interactions at 1.95 Å in [Bu_4N][**3**] and 4 Cu-N/O interactions at 1.86 Å in **4** (Table S3). The second and third shell for [Bu_4N][**3**] and **4** were fit with single and multiple-scattering components from the nitrogenous ligand (see Table S3). The ~0.1 Å shortening of the first shell Cu-N/O distances is also consistent with the oxidation of Cu(II) in [Bu_4N][**3**] to Cu(III) in **4**.

Cu K-edge XAS and EXAFS of [Bu_4N][2] and [Bu_4N][3]. Figure S9 shows a comparison of the Cu K-edge XAS spectra of [Bu_4N][**2**] and [Bu_4N][**3**]. The inset shows the second derivative of the pre-edge region. The pre-edge of both [Bu_4N][**2**] and [Bu_4N][**3**] occur at ~8979.1 eV indicating that both are Cu(II) complexes. The rising-edge spectra for the two complexes have an intense shakedown transition typical for square planar system. Figure S10 shows the k^3 weighted Cu K-edge EXAFS for [Bu_4N][**2**] along with the non-phase shift corrected Fourier transform (k=2-13.2 Å^{-1}). *FEFF* fits are presented in Table S3, which are consistent with 3 Cu-N/O at 1.96 Å and 1 Cu-Cl at 2.21 Å. The second and third shells were fit with single and multiple scattering contributions from the nitrogenous ligand system. The bond distances for [Bu_4N][**2**] and [Bu_4N][**3**] are in good agreement with those obtained from x-ray diffraction and indicate that the sample integrity is retained in solution.

Procedure for the kinetic measurements of the reaction of 4 with substrates and the product analysis: Kinetic analysis of the reaction of **4** with DHA was monitored by UV-vis spectroscopy and performed as described above, recording a spectrum every 5 seconds for reactions run at -50 °C or colder and every 3 seconds for reactions run at -40 °C or warmer. Data were collected until there was no change in the spectrum for at least 5 minutes. The kinetic trace was determined by the disappearance of the UV-vis feature due to **4** at 540 nm and was corrected for the absorbance due to the products. The extent of the reaction, λ, at time t is given by the following equation:

---

(10) Sarangi, R.; Aboelella, N.; Fujisawa, K.; Tolman, W. B.; Hedman, B.; Hodgson, K. O.; Solomon, E. I. *J. Am. Chem. Soc.* **2006**, *128*, 8286-8296.
(11) DuBois, J. L.; Mukherjee, P.; Stack, T. D. P.; Hedman, B.; Solomon, E. I.; Hodgson, K. O. *J. Am. Chem. Soc.* **2000**, *122*, 5775-5787.

$$\lambda = \frac{A_t - A_0}{A_P - A_0} \quad (1)$$

where A_t is the absorbance at time t, A_0 is the absorbance at t = 0 and A_P is the absorbance of the products at the completion of the reaction. The concentration of **4** is then determined from A_0*(1-λ) and the concentration of the products is determined from A_P* λ. The pseudo first order rate constant, k_{obs}, is determined from the decay of **4** as a function of time. Second order rate constants are determined based on the concentration of DHA ($k = k_{obs}$/[DHA]) and are used for all Eyring plots and KIE determinations.

Procedure for the reduction of LCuOH (4). Stock solutions of reagents were prepared similar to those for the oxidation: 3 mM solutions of **[Bu$_4$N][3]**, $FcPF_6$ and decamethylferrocene (Fc*) in acetone. A 0.1 mL aliquot of the stock solution of [Bu$_4$N][**3**] was added to a UV-vis cuvette along with 2.7 mL of acetone. After cooling the cuvette to -80 °C, 0.1 mL of the $FcPF_6$ solution was added, causing the immediate formation of an intensely purple species (**4**). This was then followed by the addition of 0.1 mL of the Fc* solution, which immediately quenched the purple species, forming a pale green solution. Control experiments were also done omitting each of the three reagents (replacing with an additional 0.1 mL of acetone to maintain concentration). Omitting the $FcPF_6$ yielded no reaction and omitting **[Bu$_4$N][3]** yielded a solution of Fc^{*+}. The UV-vis data are shown in Figure S13.

Procedure for assaying contamination of chloride complex [PPN][2] in crystalline [PPN][3]. Three batches (A-C) of crystalline **[PPN][3]** were prepared as described above (as used to prepare samples evaluated by X-ray crystallography). Each batch was dissolved in acetone and UV-vis spectra were compared to those of pure samples of **[Bu$_4$N][2]** and **[Bu$_4$N][3]**. The extinction values at 400 nm (which l_{max} of the former chloride complex) were measured and the data analyzed via the following equation to determine the level of chloride contamination:

$$(\varepsilon(obs)-\varepsilon(OH))/(\varepsilon(Cl)-\varepsilon(OH)) = \text{extent of chloride substitution}$$

where the ε's are the extinction values at 400 nm for the crystals (ε(obs)), **[Bu$_4$N][3]** (ε(OH)) and **[Bu$_4$N][2]** (ε(Cl)). Based on this data, the A sample was 26.8% chloride, the B sample was 28.4% chloride and the C sample was 22.3% chloride.

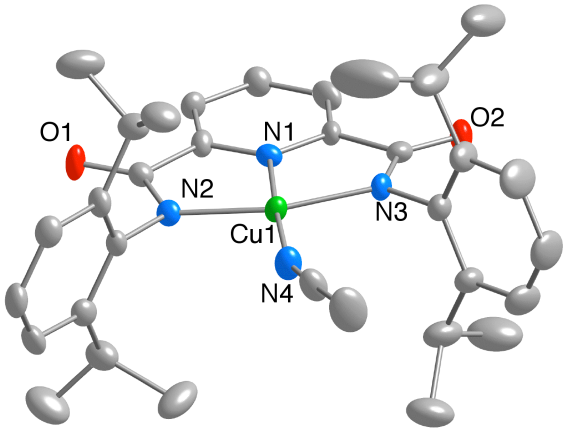

Figure S1. Representation of the X-ray crystal structure of LCu(CH_3CN) (**1**), shown as 50% thermal ellipsoids (H atoms omitted for clarity). For details, including interatomic distances and angles, see the CIF.

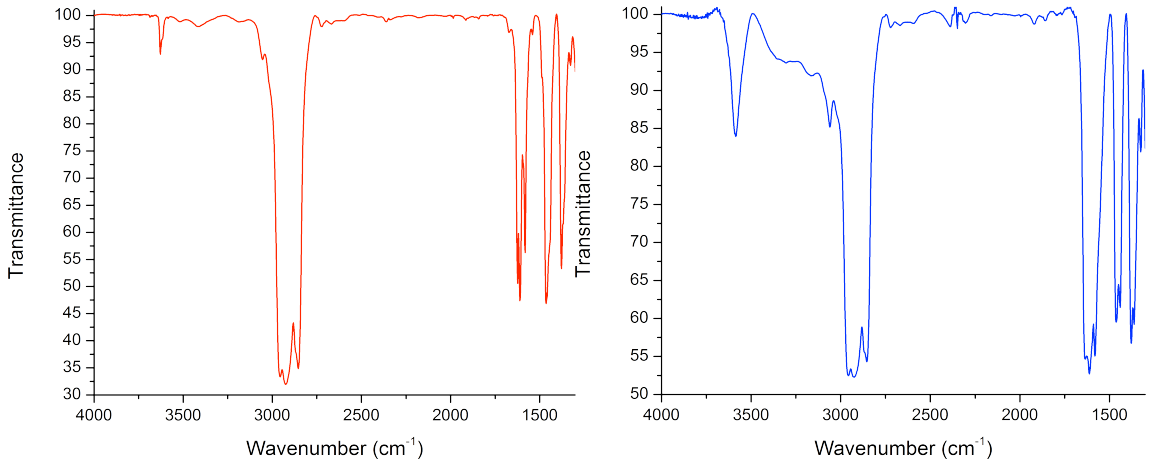

(a) (b)

Figure S2. FTIR spectra (nujol) of (a) $[Bu_4N]$[**3**] and (b) **5**.

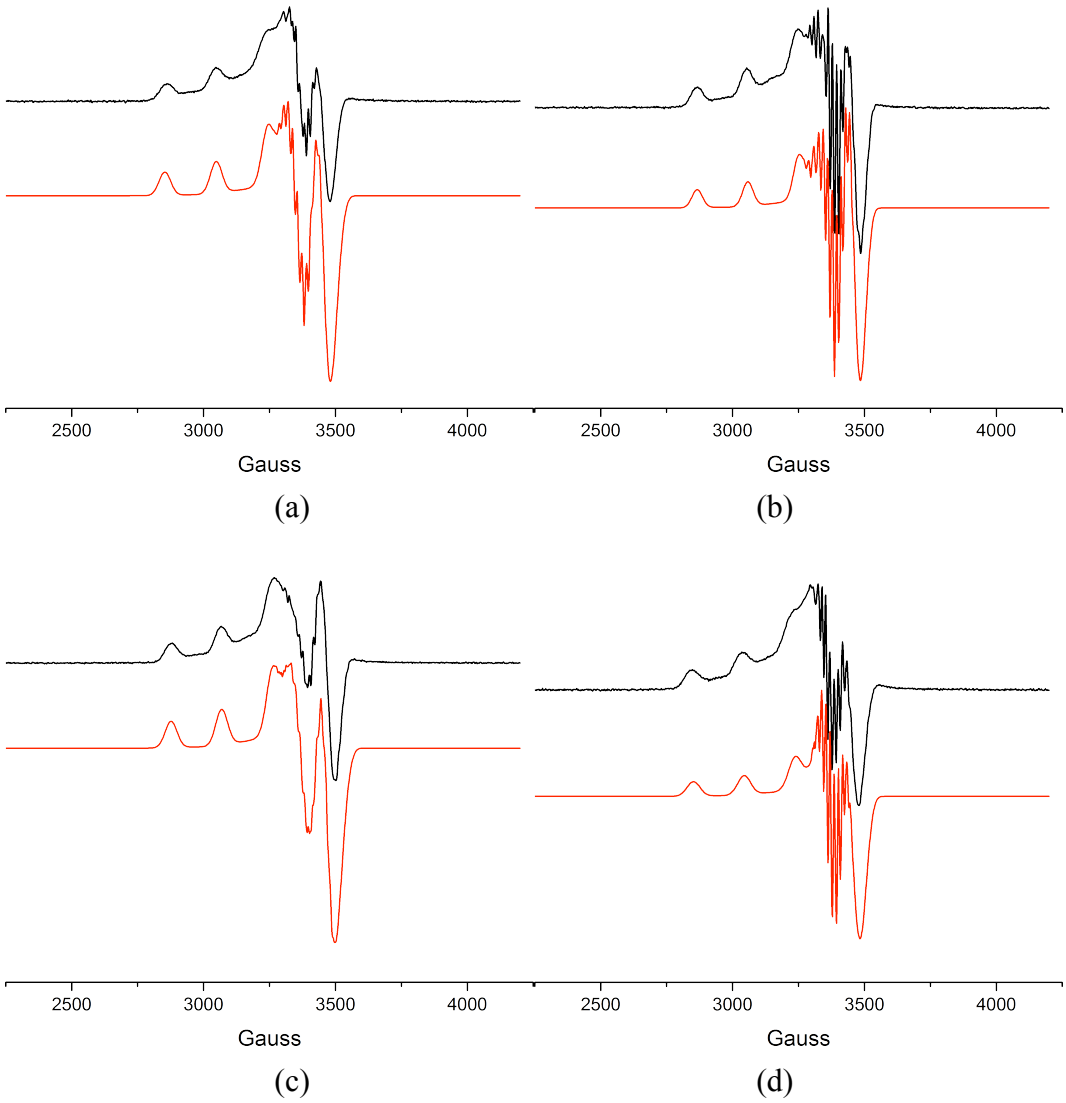

Figure S3. EPR spectra (black) and simulations (red) of (a) **1**, (b) [Bu_4N][**3**], (c) [Bu_4N][**2**], and (d) **5**. All spectra measured for solutions in 3:1 toluene/acetone.

Table S1. Summary of simulated EPR parameters (A units x 10^{-4} cm^{-1}).

Compound	**g(x)**	**g(y)**	**g(z)**	**A(Cu)**	**A(N_{amide})**	**A(N_{py})**	**A(Cl)**
1	2.027	2.064	2.190	199	18.8	14	
[Bu_4N][**2**]	2.016	2.054	2.177	195	18.2	15.3	15.3
[Bu_4N][**3**]	2.032	2.055	2.185	196	17.7	13.4	
5	2.020	2.056	2.195	197	15.8	13.0	

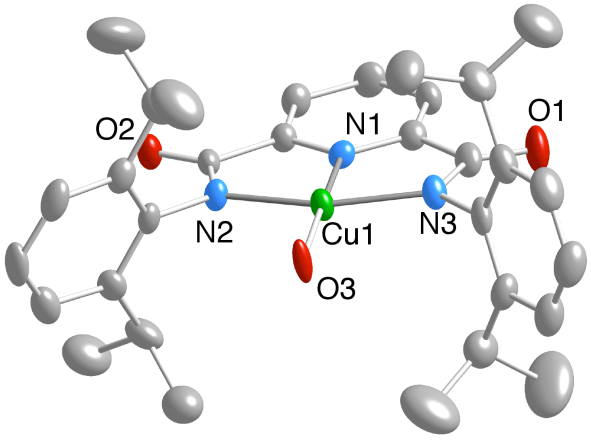

Figure S4. Representation of the X-ray crystal structure of the anionic portion of [PPN][**3**], shown as 50% thermal ellipsoids (H atoms omitted for clarity). For details, including interatomic distances and angles, see the CIF.

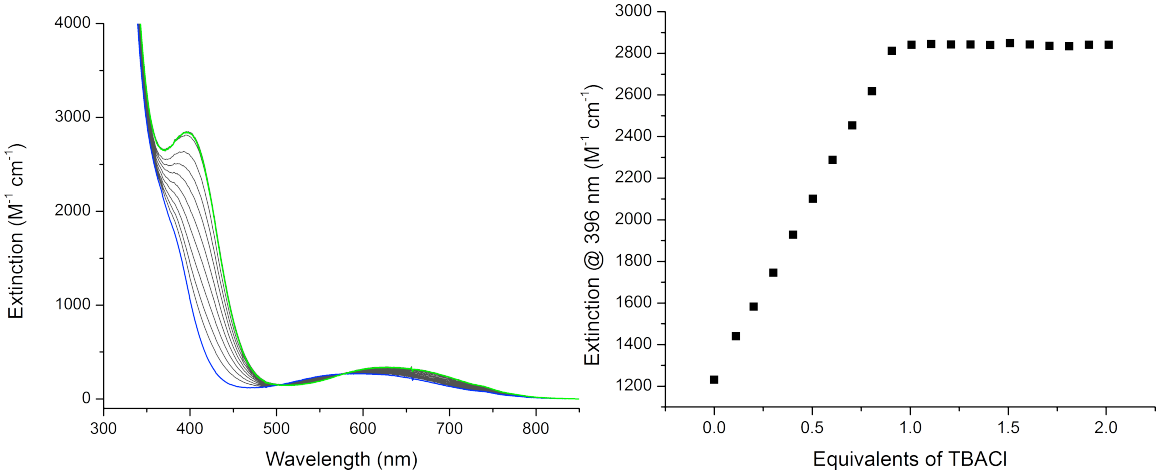

Figure S5. (left) UV-vis spectra showing the the conversion of [Bu_4N][**3**] (blue) to [Bu_4N][**2**] (green) by the addition of aliquots of Bu_4NCl in acetone at -80 °C. (right) Titration data monitoring the conversion at 396 nm, showing the completion of reaction upon addition of 1 equiv. Bu_4NCl.

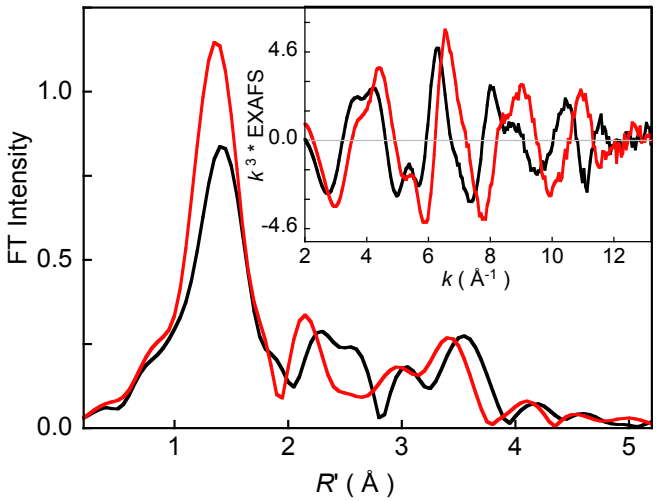

Figure S6. The k^3 weighted Cu K-edge EXAFS (inset) and their corresponding non-phase shift corrected Fourier transforms for [Bu_4N][**3**] (—) and **4** (—).

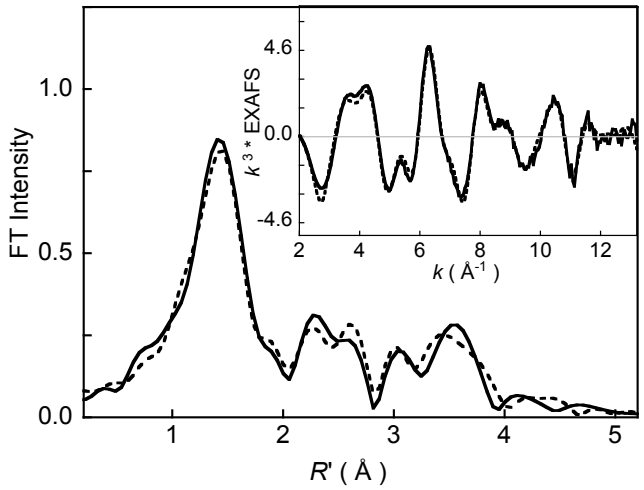

Figure S7. The k^3 weighted Cu K-edge EXAFS (inset) and their corresponding non-phase shift corrected Fourier transforms for [Bu_4N][**3**]. Data (—), Fit (– – –).

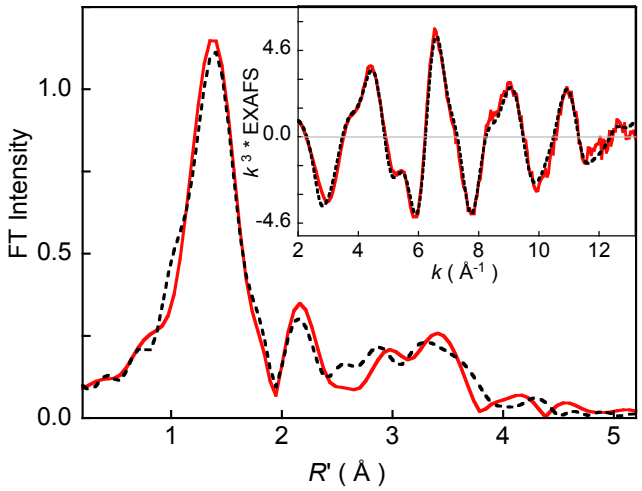

Figure S8. The k^3 weighted Cu K-edge EXAFS (inset) and their corresponding non-phase shift corrected Fourier transforms for **4**. Data (—), Fit (– – –).

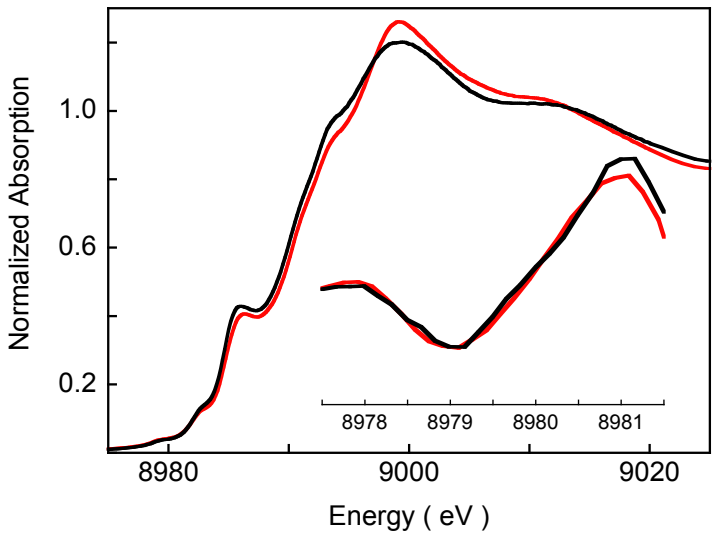

Figure S9. The normalized Cu K-edge XAS spectra of [Bu_4N][**3**] (—) and [Bu_4N][**2**] (—). The inset shows the second derivative spectra of the pre-edge region.

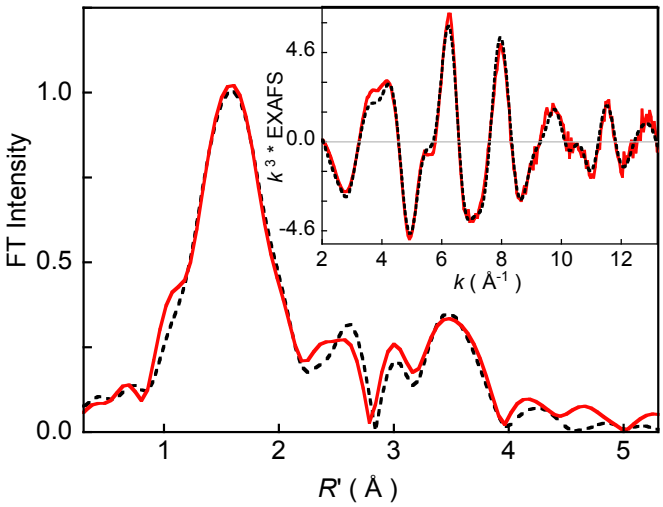

Figure S10. The k^3 weighted Cu K-edge EXAFS (inset) and their corresponding non-phase shift corrected Fourier transforms for [Bu_4N][**2**]. Data (—), Fit (−−−).

Table S2. Cu-K Pre-edge Analysis.

	Pre-edge (1s→3d) (eV)[a]	Cu K-edge Maxima (eV)
[Bu_4N][**2**]	8979.1	8999.1
[Bu_4N][**3**]	8979.1	8999.3
4	8980.8	9000.4

[a]Accuracy of measurement is <0.05 eV on SSRL beamline 7-3. Pre-edge positions estimated from second derivatives obtained in Kaleidagraph.

Table S3. EXAFS Least Squares Fitting Results

Complex	Coordination/Path	R(Å)[a]	σ^2(Å^2)[b]	E_0 (eV)	F[c]
[Bu_4N][**2**]	3 Cu-N/O	1.98	423	-6.94	0.13
	1 Cu-Cl	2.21	272		
	4 Cu-C	2.85	315		
	2 Cu-C	3.06	207		
	12 Cu-C-N	3.07	395		
	16 Cu-C-N	4.17	275		
	12 Cu-C-N	4.76	949		
[Bu_4N][**3**]	4 Cu-N/O	1.95	737	-6.47	0.12
	4 Cu-C	2.85	359		
	2 Cu-C	3.07	586		
	12 Cu-C-N	3.10	912		
	16 Cu-C-N	4.18	467		
	12 Cu-C-N	4.67	1139		

4	4 Cu-N/O	1.86	537	-7.71	0.16
	4 Cu-C	2.75	323		
	2 Cu-C	2.94	317		
	12 Cu-C-N	3.01	222		
	16 Cu-C-N	4.05	565		
	12 Cu-C-N	4.54	1180		

[a]The estimated standard deviations for the distances are in the order of ± 0.02 Å. [b]The σ^2 values are multiplied by 10^5. [c]Error is given by $\Sigma[(\chi_{obsd} - \chi_{calcd})^2 k^6]/\Sigma[(\chi_{obsd})^2 k^6]$. [d]The σ^2 factor of the multiple scattering path is linked to that of the corresponding single scattering path.

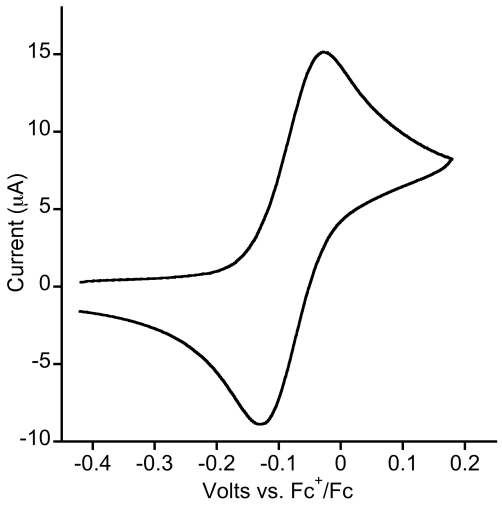

Figure S11. Cyclic voltammogram of [Bu_4N][**3**] in acetone (0.1 M Bu_4NPF_6).

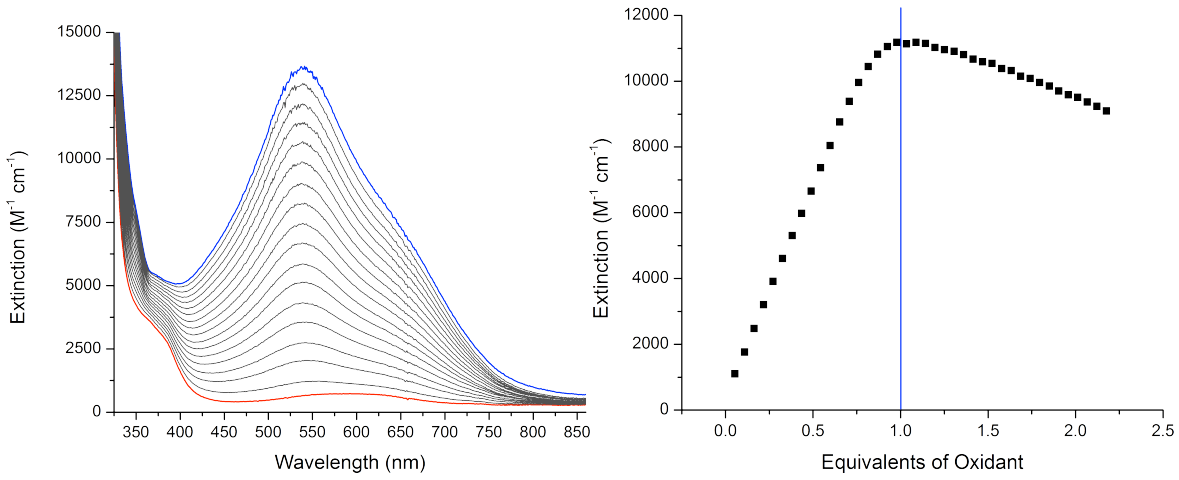

(a) (b)

Figure S12. Titration data for reaction of [Bu_4N][**3**] with $Fc^+PF_6^-$ at −80 °C. (a) UV-vis spectroscopic changes as equivalents of $Fc^+PF_6^-$ are added to [Bu_4N][**3**] (red = starting spectrum, blue = ending spectrum). (b) Extinction at 540 nm as a function of equiv oxidant added to [Bu_4N][**3**].

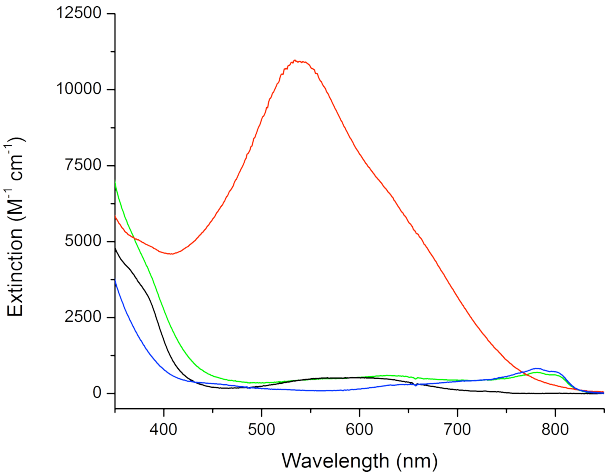

Figure S13. UV-vis spectra in acetone at -80 °C of [Bu_4N][**3**] (black), the product of reaction with $FcPF_6$, **4** (red), after subsequent reduction with Fc* (green), and the control spectrum of $FcPF_6$ + Fc* (blue).

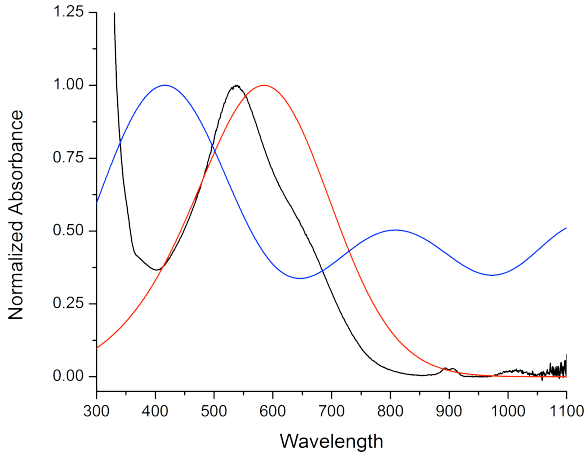

Figure S14. Calculated UV-vis spectra from TD-DFT calculations for **4**. Spectra shown are experimental (black), singlet state (red) and triplet state (blue).

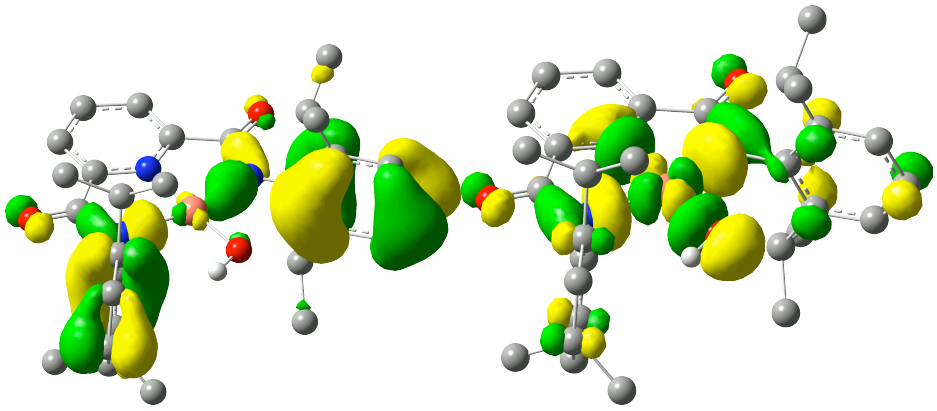

(a) (b)

Figure S15. TD-DFT orbitals involved in the calculated transition at 589 nm. The transition is from (a) to (b).

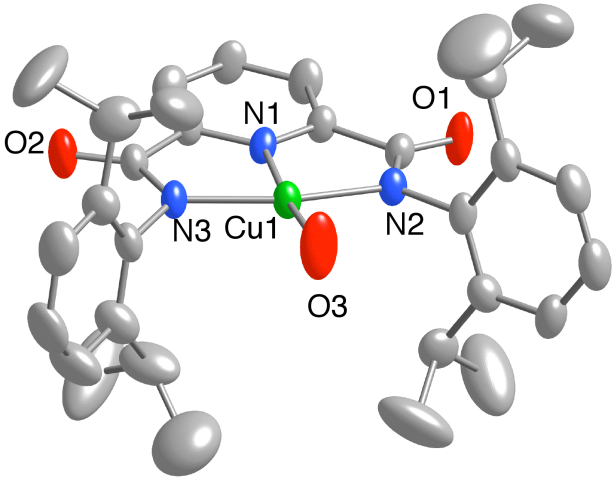

Figure S16. Representation of the X-ray crystal structure of **5**, shown as 50% thermal ellipsoids (H atoms omitted for clarity). For details, including interatomic distances and angles, see the CIF.

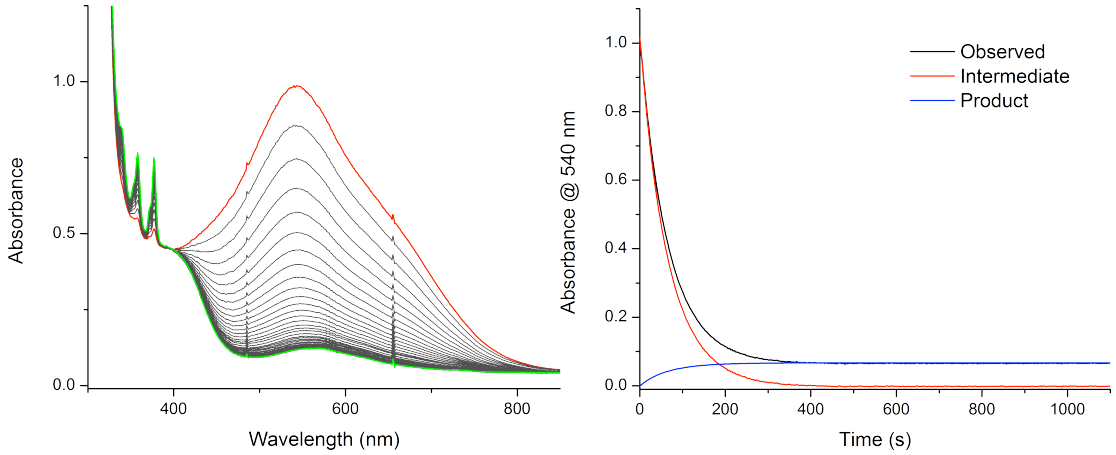

Figure S17. (left) Change in the UV-vis spectrum of **4** (red to green) in the presence of 10 equivalents of DHA in acetone at -40 °C. (right) Representative deconvolution of the observed absorbance at 540 nm (black) into components **4** (red) and **5** (blue). Rate constants were determined by modeling the rate of decay of the red curve.

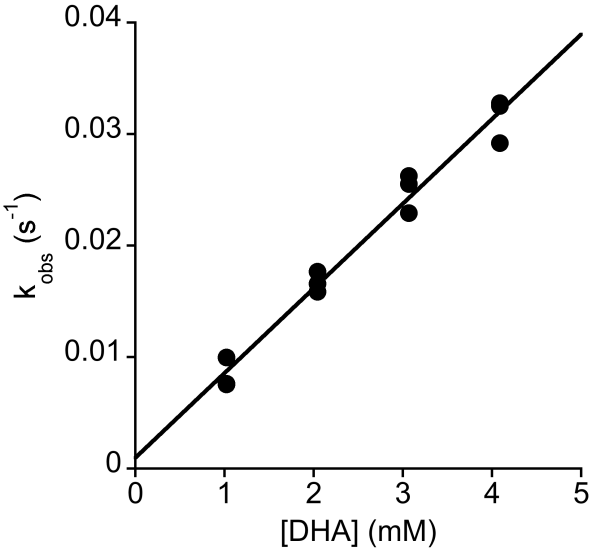

Figure S18. Linear relationship between pseudo first order rate constant (k_{obs}, three replicates) and the initial concentration of DHA (10-40 equivalents used, based on 0.1 mM Cu in the reaction). Reactions were performed at -60 °C in acetone. Regression equation: $k_{obs} = 7.66 \times 10^{-3}$ [DHA] + 9.07×10^{-4} ($r^2 = 0.996$). The initial rate of the decay of **4** was measured at -80 °C and found to proceed with a rate constant of 1.35×10^{-4} M^{-1} s^{-1} which agrees with the intercept of the regression function.

Table S4. Rate constants used to construct the Eyring plot (Figure 4 in text).

Temp. (°C)	k_H Run 1	k_H Run 2	k_H Run 3	Average	Std Dev
-30	24.56282	24.41563	23.50446	24.2	0.57
-40	14.82068	14.01603	13.12566	14.0	0.85
-50	7.02495	9.24107	8.68149	8.3	1.15
-60	4.02513	4.17551	5.28693	4.5	0.69
-70	2.3145	1.95966	2.18854	2.2	0.17
-80	1.04511	1.01551	1.12631	1.06	0.057
	Regression equation: ln(k/T) = -2713.3 (1/T) + 8.839			$r^2 = 0.9998$	
	k_D Run 1	k_D Run 2	k_D Run 3	Average	Std Dev
-30	0.69193	0.58284	0.62588	0.63	0.055
-40	0.3187	0.33527	0.33405	0.329	0.0092
-50	0.18412	0.21211	0.17629	0.19	0.019
-60	0.07303	0.06489	0.07075	0.069	0.0042
-70	0.04916	0.05111	-----	0.050	0.0014
	Regression equation: ln(k/T) = -2827.5 (1/T) + 5.559			$r^2 = 0.981$	

[a] For k_H runs, 10 equiv DHA used. For k_D runs, 200 equiv DHA-d_4 used. All units for k values are $M^{-1}s^{-1}$.

Computational Details

DFT geometry optimizations were performed on complexes of the full, untruncated ligand using the mPW functional[12] implemented in Gaussian09.[13] A mixed basis set comprised of 6-311+g(d,p) on C, H, N and O and the Stuttgart/Dresden basis set and pseudopotential (SDD) on Cu (including 2 f-functions with coefficients 5.208 and 1.315). Final optimizations were performed with no frozen coordinates. Solvation effects were included by performing single point energies on optimized structures using the SMD solvation model in acetone. Energy minima and transition states were identified though frequency analysis. Time dependant DFT (TDDFT) calculations were performed using the B98 functional[14] in Gaussian09 with the 6-31+G(d,p) basis sets on C, H, N and O and the SDD basis set/pseudopotential as previously described on Cu.

The structure of **3**$^-$ and singlet state of **4** were located in the Cs space group with the hydroxide hydrogen coplanar with the ligand as the lowest energy structure. The triplet state of **4** distorted from a square planar structure with the hydroxide ~10 degrees out of the square plane; however it could only be located as a rotational transition state with the hydroxide hydrogen perpendicular to the ligand plane. This transition state was also located for **3**$^-$ and the singlet state of **4** where it was found that the rotational barrier was fairly small on the scale of the calculated singlet/triplet energy gap.

Table S5. Summary of Energetic Results

Structure	Relative Gas Phase G	Relative Solvated G
3$^-$ $[LCuOH]^-$ doublet	---	---
3$^-$ $[LCuOH]^-$ doublet TS	2.7 kcal/mol	3.5 kcal/mol
4 LCuOH singlet	---	---
4 LCuOH singlet TS	2.5 kcal/mol	2.0 kcal/mol
4 LCuOH triplet TS	19.9 kcal/mol	21.0 kcal/mol

TDDFT Transitions

UV-vis transition energies were calculated for the first 36 states for both the singlet and triplet wavefunctions as described above. Key transitions are bolded and described below.

(12) (a) Perdew, J. P. Unified Theory of Exchange and Correlation Beyond the Local Density Approximation. *In Electronic Structure of Solids '91*; Ziesche, P., Eschrig, H., Eds.; Akademie Verlag: Berlin, 1991, pp 11-20; (b) Perdew, J.; Wang, Y. *Phys. Rev. B* **1992**, *45*, 13244-13249. (c) Adamo, C.; Barone, V. *J. Chem. Phys*. **1998**, *108*, 664-675.

(13) M. J. Frisch, G. W. Trucks, H. B. Schlegel, G. E. Scuseria, M. A. Robb, J. R. Cheeseman, G. Scalmani, V. Barone, B. Mennucci, G. A. Petersson, H. Nakatsuji, M. Caricato, X. Li, H. P. Hratchian, A. F. Izmaylov, J. Bloino, G. Zheng, J. L. Sonnenberg, M. Hada, M. Ehara, K. Toyota, R. Fukuda, J. Hasegawa, M. Ishida, T. Nakajima, Y. Honda, O. Kitao, H. Nakai, T. Vreven, J. A. Montgomery, Jr., J. E. Peralta, F. Ogliaro, M. Bearpark, J. J. Heyd, E. Brothers, K. N. Kudin, V. N. Staroverov, R. Kobayashi, J. Normand, K. Raghavachari, A. Rendell, J. C. Burant, S. S. Iyengar, J. Tomasi, M. Cossi, N. Rega, J. M. Millam, M. Klene, J. E. Knox, J. B. Cross, V. Bakken, C. Adamo, J. Jaramillo, R. Gomperts, R. E. Stratmann, O. Yazyev, A. J. Austin, R. Cammi, C. Pomelli, J. W. Ochterski, R. L. Martin, K. Morokuma, V. G. Zakrzewski, G. A. Voth, P. Salvador, J. J. Dannenberg, S. Dapprich, A. D. Daniels, O. Farkas, J. B. Foresman, J. V. Ortiz, J. Cioslowski, D. J. Fox, *Gaussian 09*, Revision A.02; Gaussian, Inc.: Wallingford CT, 2009.

([14]) (a) Becke, A. D. *J. Chem. Phys.* **1997**, *107*, 8554-8560. (b) Schmider, H. L; Becke, A. D. *J. Chem. Phys.* **1998**, *108*, 9624-9631. (c) Cramer, C. J.; Truhlar, D. G. *Phys. Chem. Chem. Phys*. **2009**, *11*, 10757-10816.

Transitions were then fit to standard Gaussian curves to determine the calculated spectra shown above.

Table S6. LCuOH singlet

Energy (nm)	Oscillator Strength	Description	Energy (nm)	Oscillator Strength	Description
1053.63	0		441.93	0	
1007.75	0		435.53	0.0014	
894.65	0		426.14	0.0231	
821.04	0		422.51	0	
707.43	0.0212		418.82	0	
674.29	0.0208		399.90	0	
640.91	0		382.93	0	
630.80	0		382.03	0.0002	
625.11	0		381.60	0	
600.40	0.0076		381.51	0	
598.78	0.0016		378.26	0	
589.55	**0.2892**	**LMCT**	377.85	0.0008	
559.34	0.002		374.80	0	
544.61	0		373.22	0.0055	
480.02	0.0414		366.08	0	
474.57	0		364.88	0.0056	
457.14	0		362.69	0.0002	
442.65	0		356.65	0.0019	

Table S7. LCuOH triplet

Energy (nm)	Oscillator Strength	Description	Energy (nm)	Oscillator Strength	Description
2729.45	0.0004		443.86	0.0007	
2323.03	**0.0884**		443.73	0.0017	
1382.7	0.004		416.12	0.0008	
1345.44	0.0002		412.93	0.0004	
1286.5	0.006		412.5	0.0031	
1126.52	**0.0349**		405.92	0	
870.7	0.0202		401.02	0.0066	
781.68	0.0051		389.12	0.0043	
742.5	**0.017**		383.45	0.001	
678.8	0.0004		372.71	0.0032	
529.09	0.0015		372.23	0.0024	
511.29	0.0001		371.21	0.005	
491.11	0.0031		370.44	0.001	
484.38	0.0007		362.33	0.0018	
479.68	**0.0142**		360.67	0.0021	
467.34	0.0023		356.79	0.0055	

461.97	0.0008		352.25	0.0084	
452.58	0.01		345.56	0	

Optimized geometries

```
LCuOH doublet, rotational transition state
Cu      0.111431     0.172982     0.000000
 O      1.533792    -1.053514     0.000000
 N     -1.123514     1.692277     0.000000
 O     -1.362994     1.829806     3.535274
 C     -1.527091     2.191782     1.176774
 C     -2.382319     3.297777     1.215241
 H     -2.694214     3.682972     2.185498
 C     -2.803466     3.853979     0.000000
 H     -3.469777     4.719297     0.000000
 C     -2.382319     3.297777    -1.215241
 H     -2.694214     3.682972    -2.185498
 C     -1.527091     2.191782    -1.176774
 C     -1.017895     1.447759     2.396799
 N     -0.229777     0.404577     2.047100
 C      0.288046    -0.440364     3.061533
 C     -0.502678    -1.506542     3.570117
 C      0.047294    -2.355859     4.541104
 H     -0.557147    -3.173212     4.942066
 C      1.352256    -2.177428     5.006009
 H      1.764858    -2.850013     5.761368
 C      2.125158    -1.133760     4.493073
 H      3.148480    -0.997521     4.851397
 C      1.616988    -0.256196     3.524727
 C     -1.935641    -1.723032     3.094556
 H     -2.085504    -1.064092     2.226904
 C     -2.949639    -1.302115     4.179305
 H     -2.777089    -0.260613     4.481882
 H     -2.857828    -1.941949     5.071981
 H     -3.982083    -1.392639     3.803758
 C     -2.189984    -3.168230     2.624060
 H     -1.476159    -3.463678     1.841762
 H     -3.207330    -3.264797     2.212917
 H     -2.099023    -3.889198     3.451565
 C      2.491083     0.871891     2.990734
 H      1.888097     1.415575     2.249810
 C      2.873592     1.869222     4.103219
 H      1.977934     2.275228     4.594770
 H      3.450343     2.709738     3.684632
 H      3.496711     1.390345     4.875592
 C      3.731240     0.323148     2.258864
 H      4.323309     1.149231     1.832329
 H      3.415015    -0.342615     1.443415
```

```
 H     4.386766    -0.237571     2.945084
 N    -0.229777     0.404577    -2.047100
 O    -1.362994     1.829806    -3.535274
 C    -1.017895     1.447759    -2.396799
 C     0.288046    -0.440364    -3.061533
 C    -0.502678    -1.506542    -3.570117
 C     0.047294    -2.355859    -4.541104
 H    -0.557147    -3.173212    -4.942066
 C     1.352256    -2.177428    -5.006009
 H     1.764858    -2.850013    -5.761368
 C     2.125158    -1.133760    -4.493073
 H     3.148480    -0.997521    -4.851397
 C     1.616988    -0.256196    -3.524727
 C    -1.935641    -1.723032    -3.094556
 H    -2.085504    -1.064092    -2.226904
 C    -2.189984    -3.168230    -2.624060
 H    -1.476159    -3.463678    -1.841762
 H    -2.099023    -3.889198    -3.451565
 H    -3.207330    -3.264797    -2.212917
 C    -2.949639    -1.302115    -4.179305
 H    -2.777089    -0.260613    -4.481882
 H    -3.982083    -1.392639    -3.803758
 H    -2.857828    -1.941949    -5.071981
 C     2.491083     0.871891    -2.990734
 H     1.888097     1.415575    -2.249810
 C     3.731240     0.323148    -2.258864
 H     3.415015    -0.342615    -1.443415
 H     4.323309     1.149231    -1.832329
 H     4.386766    -0.237571    -2.945084
 C     2.873592     1.869222    -4.103219
 H     1.977934     2.275228    -4.594770
 H     3.496711     1.390345    -4.875592
 H     3.450343     2.709738    -3.684632
 H     1.202931    -1.965516     0.000000

LCuOH doublet, rotational minimum
Cu     0.097033     0.036832     0.000000
 O    -1.764073     0.129288     0.000000
 N     2.043270     0.002746     0.000000
 O     2.228999    -3.540845     0.000000
 C     2.666088    -1.185730     0.000000
 C     4.062754    -1.247236     0.000000
 H     4.543660    -2.224898     0.000000
 C     4.780636    -0.043198     0.000000
 H     5.872546    -0.061517     0.000000
 C     4.103054     1.183499     0.000000
 H     4.614826     2.145426     0.000000
```

C	2.704653	1.169669	0.000000
C	1.743493	-2.389034	0.000000
N	0.442362	-2.014489	0.000000
C	-0.572589	-3.004030	0.000000
C	-1.105379	-3.472025	1.232530
C	-2.140979	-4.417453	1.206632
H	-2.551954	-4.787591	2.148455
C	-2.658197	-4.894285	0.000000
H	-3.465303	-5.630090	0.000000
C	-2.140979	-4.417453	-1.206632
H	-2.551954	-4.787591	-2.148455
C	-1.105379	-3.472025	-1.232530
C	-0.532637	-2.987888	2.559821
H	0.045473	-2.078603	2.337853
C	0.445112	-4.031377	3.143232
H	1.230884	-4.278465	2.416526
H	-0.086657	-4.961448	3.402296
H	0.921731	-3.647219	4.059755
C	-1.618146	-2.606302	3.582427
H	-2.307814	-1.857678	3.168128
H	-1.154783	-2.178904	4.485276
H	-2.209907	-3.479095	3.900764
C	-0.532637	-2.987888	-2.559821
H	0.045473	-2.078603	-2.337853
C	0.445112	-4.031377	-3.143232
H	1.230884	-4.278465	-2.416526
H	0.921731	-3.647219	-4.059755
H	-0.086657	-4.961448	-3.402296
C	-1.618146	-2.606302	-3.582427
H	-1.154783	-2.178904	-4.485276
H	-2.307814	-1.857678	-3.168128
H	-2.209907	-3.479095	-3.900764
N	0.510169	2.073018	0.000000
O	2.352507	3.535838	0.000000
C	1.823061	2.404841	0.000000
C	-0.463082	3.104173	0.000000
C	-0.972413	3.595932	1.230127
C	-1.963242	4.587508	1.205880
H	-2.361808	4.969090	2.149134
C	-2.456135	5.091045	0.000000
H	-3.227928	5.864124	0.000000
C	-1.963242	4.587508	-1.205880
H	-2.361808	4.969090	-2.149134
C	-0.972413	3.595932	-1.230127
C	-0.499860	3.020892	2.560010
H	0.358831	2.371344	2.339219
C	-1.599597	2.133541	3.180376

```
 H    -1.909168     1.355941     2.467275
 H    -2.487017     2.732522     3.441741
 H    -1.236154     1.648035     4.100999
 C    -0.019595     4.106656     3.541096
 H     0.776357     4.717738     3.092153
 H     0.376075     3.645110     4.460076
 H    -0.839272     4.780061     3.838142
 C    -0.499860     3.020892    -2.560010
 H     0.358831     2.371344    -2.339219
 C    -1.599597     2.133541    -3.180376
 H    -1.909168     1.355941    -2.467275
 H    -1.236154     1.648035    -4.100999
 H    -2.487017     2.732522    -3.441741
 C    -0.019595     4.106656    -3.541096
 H     0.776357     4.717738    -3.092153
 H    -0.839272     4.780061    -3.838142
 H     0.376075     3.645110    -4.460076
 H    -2.113050    -0.778119     0.000000

LCuOH restricted singlet, rotational transition state
Cu    -0.047838     0.248997     0.000000
 O     1.163534    -1.114640     0.000000
 N    -1.112884     1.796727     0.000000
 O    -1.204302     1.859194     3.521809
 C    -1.462296     2.316182     1.180830
 C    -2.232364     3.479641     1.218556
 H    -2.512609     3.896263     2.185428
 C    -2.613633     4.060034     0.000000
 H    -3.215001     4.970050     0.000000
 C    -2.232364     3.479641    -1.218556
 H    -2.512609     3.896263    -2.185428
 C    -1.462296     2.316182    -1.180830
 C    -0.958255     1.518786     2.361391
 N    -0.241230     0.424939     1.947585
 C     0.299288    -0.490034     2.882998
 C    -0.503211    -1.570293     3.346557
 C     0.051901    -2.454528     4.279333
 H    -0.549741    -3.281754     4.659684
 C     1.362729    -2.294921     4.736072
 H     1.776043    -2.996741     5.462519
 C     2.144481    -1.240547     4.260602
 H     3.168275    -1.127805     4.621162
 C     1.639554    -0.326171     3.327779
 C    -1.945631    -1.752361     2.888974
 H    -2.108104    -1.071284     2.040127
 C    -2.931392    -1.345196     4.006085
 H    -2.743761    -0.317336     4.343624
```

H	-2.833233	-2.012318	4.876087
H	-3.969864	-1.411274	3.646647
C	-2.231505	-3.183542	2.393986
H	-1.532669	-3.484951	1.600565
H	-3.253607	-3.250088	1.992247
H	-2.150785	-3.919954	3.207108
C	2.512812	0.820085	2.837902
H	1.956686	1.337168	2.042727
C	2.770421	1.841483	3.966526
H	1.827452	2.221324	4.383170
H	3.350629	2.695600	3.585083
H	3.344751	1.387386	4.788373
C	3.831224	0.313471	2.221712
H	4.405295	1.155720	1.806769
H	3.630509	-0.403039	1.414467
H	4.466946	-0.179513	2.972629
N	-0.241230	0.424939	-1.947585
O	-1.204302	1.859194	-3.521809
C	-0.958255	1.518786	-2.361391
C	0.299288	-0.490034	-2.882998
C	-0.503211	-1.570293	-3.346557
C	0.051901	-2.454528	-4.279333
H	-0.549741	-3.281754	-4.659684
C	1.362729	-2.294921	-4.736072
H	1.776043	-2.996741	-5.462519
C	2.144481	-1.240547	-4.260602
H	3.168275	-1.127805	-4.621162
C	1.639554	-0.326171	-3.327779
C	-1.945631	-1.752361	-2.888974
H	-2.108104	-1.071284	-2.040127
C	-2.231505	-3.183542	-2.393986
H	-1.532669	-3.484951	-1.600565
H	-2.150785	-3.919954	-3.207108
H	-3.253607	-3.250088	-1.992247
C	-2.931392	-1.345196	-4.006085
H	-2.743761	-0.317336	-4.343624
H	-3.969864	-1.411274	-3.646647
H	-2.833233	-2.012318	-4.876087
C	2.512812	0.820085	-2.837902
H	1.956686	1.337168	-2.042727
C	3.831224	0.313471	-2.221712
H	3.630509	-0.403039	-1.414467
H	4.405295	1.155720	-1.806769
H	4.466946	-0.179513	-2.972629
C	2.770421	1.841483	-3.966526
H	1.827452	2.221324	-4.383170
H	3.344751	1.387386	-4.788373

```
 H     3.350629     2.695600    -3.585083
 H     0.694569    -1.966853     0.000000

LCuOH restricted singlet, rotational minium
Cu     0.248634     0.018531     0.000000
 O    -1.558305     0.118895     0.000000
 N     2.120167     0.014824     0.000000
 O     2.191171    -3.509999     0.000000
 C     2.738533    -1.171142     0.000000
 C     4.133248    -1.216839     0.000000
 H     4.630651    -2.186151     0.000000
 C     4.835019    -0.002084     0.000000
 H     5.925730    -0.008870     0.000000
 C     4.148228     1.220973     0.000000
 H     4.657160     2.184297     0.000000
 C     2.752830     1.192568     0.000000
 C     1.785856    -2.344305     0.000000
 N     0.480485    -1.919949     0.000000
 C    -0.587511    -2.858365     0.000000
 C    -1.121992    -3.308334     1.239770
 C    -2.179027    -4.228107     1.209421
 H    -2.597162    -4.594716     2.148161
 C    -2.704598    -4.687006     0.000000
 H    -3.528054    -5.403138     0.000000
 C    -2.179027    -4.228107    -1.209421
 H    -2.597162    -4.594716    -2.148161
 C    -1.121992    -3.308334    -1.239770
 C    -0.541852    -2.853880     2.573535
 H     0.125978    -2.004820     2.365966
 C     0.312773    -3.975839     3.203576
 H     1.099705    -4.310456     2.514455
 H    -0.310275    -4.847282     3.456738
 H     0.788032    -3.621197     4.130938
 C    -1.623839    -2.360433     3.552871
 H    -2.231006    -1.559328     3.109150
 H    -1.154779    -1.966702     4.466792
 H    -2.301075    -3.172220     3.857308
 C    -0.541852    -2.853880    -2.573535
 H     0.125978    -2.004820    -2.365966
 C     0.312773    -3.975839    -3.203576
 H     1.099705    -4.310456    -2.514455
 H     0.788032    -3.621197    -4.130938
 H    -0.310275    -4.847282    -3.456738
 C    -1.623839    -2.360433    -3.552871
 H    -1.154779    -1.966702    -4.466792
 H    -2.231006    -1.559328    -3.109150
 H    -2.301075    -3.172220    -3.857308
```

N	0.505373	1.963058	0.000000
O	2.233402	3.536700	0.000000
C	1.813544	2.376526	0.000000
C	-0.567707	2.878800	0.000000
C	-1.107420	3.323273	1.240000
C	-2.158726	4.246338	1.210483
H	-2.579724	4.610760	2.149035
C	-2.680345	4.709014	0.000000
H	-3.501355	5.428177	0.000000
C	-2.158726	4.246338	-1.210483
H	-2.579724	4.610760	-2.149035
C	-1.107420	3.323273	-1.240000
C	-0.550993	2.844828	2.573683
H	0.175953	2.048505	2.357575
C	-1.648195	2.235342	3.468116
H	-2.177097	1.428076	2.943919
H	-2.390073	2.989294	3.771172
H	-1.204536	1.822611	4.386768
C	0.203007	3.979611	3.299591
H	1.001849	4.392526	2.668718
H	0.654077	3.605698	4.231530
H	-0.479426	4.801704	3.564028
C	-0.550993	2.844828	-2.573683
H	0.175953	2.048505	-2.357575
C	-1.648195	2.235342	-3.468116
H	-2.177097	1.428076	-2.943919
H	-1.204536	1.822611	-4.386768
H	-2.390073	2.989294	-3.771172
C	0.203007	3.979611	-3.299591
H	1.001849	4.392526	-2.668718
H	-0.479426	4.801704	-3.564028
H	0.654077	3.605698	-4.231530
H	-1.915121	-0.789350	0.000000

LCuOH triplet, rotational transition state

Cu	0.245513	-0.326812	0.000000
O	1.860045	0.563746	0.000000
N	-1.282364	-1.561617	0.000000
O	-1.569904	-1.606864	3.524190
C	-1.776381	-1.981553	1.172271
C	-2.813248	-2.917610	1.213381
H	-3.194947	-3.238414	2.181827
C	-3.324428	-3.394933	0.000000
H	-4.131845	-4.128364	0.000000
C	-2.813248	-2.917610	-1.213381
H	-3.194947	-3.238414	-2.181827
C	-1.776381	-1.981553	-1.172271

C	-1.172850	-1.319763	2.386033
N	-0.173876	-0.445064	2.060118
C	0.366728	0.425739	3.015574
C	1.728514	0.242724	3.416296
C	2.269838	1.131318	4.347687
H	3.301195	1.002542	4.677048
C	1.509691	2.182374	4.874995
H	1.954564	2.865467	5.600609
C	0.183508	2.359231	4.472100
H	-0.395212	3.186330	4.887157
C	-0.413980	1.502267	3.541588
C	2.524898	-0.947984	2.906328
H	2.114426	-1.200327	1.918157
C	2.308511	-2.165950	3.834697
H	1.241797	-2.397499	3.957919
H	2.726689	-1.971146	4.834303
H	2.811755	-3.054197	3.423112
C	4.021334	-0.654976	2.716425
H	4.173418	0.215913	2.065015
H	4.510922	-1.519349	2.244241
H	4.536640	-0.475698	3.672453
C	-1.851036	1.755927	3.103930
H	-2.101092	1.017898	2.328665
C	-2.837206	1.555279	4.273143
H	-2.737387	0.547753	4.697174
H	-3.873203	1.686322	3.925285
H	-2.659123	2.288227	5.074597
C	-2.014442	3.152669	2.468145
H	-3.042852	3.285945	2.100329
H	-1.327690	3.292590	1.621085
H	-1.816093	3.953188	3.196062
N	-0.173876	-0.445064	-2.060118
O	-1.569904	-1.606864	-3.524190
C	-1.172850	-1.319763	-2.386033
C	0.366728	0.425739	-3.015574
C	1.728514	0.242724	-3.416296
C	2.269838	1.131318	-4.347687
H	3.301195	1.002542	-4.677048
C	1.509691	2.182374	-4.874995
H	1.954564	2.865467	-5.600609
C	0.183508	2.359231	-4.472100
H	-0.395212	3.186330	-4.887157
C	-0.413980	1.502267	-3.541588
C	2.524898	-0.947984	-2.906328
H	2.114426	-1.200327	-1.918157
C	4.021334	-0.654976	-2.716425
H	4.173418	0.215913	-2.065015

H	4.536640	-0.475698	-3.672453
H	4.510922	-1.519349	-2.244241
C	2.308511	-2.165950	-3.834697
H	1.241797	-2.397499	-3.957919
H	2.811755	-3.054197	-3.423112
H	2.726689	-1.971146	-4.834303
C	-1.851036	1.755927	-3.103930
H	-2.101092	1.017898	-2.328665
C	-2.014442	3.152669	-2.468145
H	-1.327690	3.292590	-1.621085
H	-3.042852	3.285945	-2.100329
H	-1.816093	3.953188	-3.196062
C	-2.837206	1.555279	-4.273143
H	-2.737387	0.547753	-4.697174
H	-2.659123	2.288227	-5.074597
H	-3.873203	1.686322	-3.925285
H	1.753246	1.530210	0.000000